Distributed Link-Layer Control for Automated Highway Systems

Huei Peng
Department of Mechanical Engineering and Applied Mechanics,
University of Michigan,
Ann Arbor, MI 48109-2125

The modeling and design of a link-layer control algorithm for automated highway systems are presented in this paper. Link-layer control systems address the coordination of traffic on a stretch of highway, and serve as the intermediate layer between traffic management (ATMS) and vehicle control (AVCS) systems. The key role of the link layer control system is to use macroscopic traffic information for improved traffic flow. A distributed control algorithm is developed based on optimal control theory. The proposed control law is implemented in a simulation program which keeps track of the motions of each individual vehicles on the highway. Simulation results under three perturbed conditions—uneven traffic distribution, broken vehicle, and traffic merging—are presented.

1 Introduction

The control design of Intelligent Transportation Systems (ITS) has attracted a lot of attention in recent years. Similar to the evolutionary development of systems with comparable complexity, top-down approaches have been undertaken for the overall structure design. Components and subsystems, in the meantime, have been developed and analyzed from bottom up. Most of the system architecture designs proposed in the past perceive layered control architecture and the control design problem is decomposed into sub-tasks. At the top, a network level controller is perceived to perform vehicle routing and scheduling. Under the network level are a group of regional-level (terminology used by Fenton et al., 1980) or link-layer (Varaiya and Shladover, 1991) control systems which supervise the operations of the traffic on a stretch of highway, and coordinate the operations of the sectors in this region (link). Each region is then further divided into sectors, in each of which a sector-level computer transmits trajectory command and monitors the operations of individual vehicles. At the lowest functional level, the vehicle-level (Fenton) or regulation layer (Varaiya and Shladover) control systems equipped on each vehicle manipulate the throttle, brake and steering to follow the assigned trajectory as close as possible. Past ITS research has focused on the network-level (ATMS) and vehicle-level (AVCS, e.g., Fenton et al., 1976; Hedrick et al., 1991; Peng and Tomizuka, 1993). This paper addresses the control problem at the link-layer level (regional level), which has not received much attention in the past.

The functional relationship among network-layer, link-layer, and regulation-layer control systems is as following: the network-layer control system (ATMS) performs route assignment to vehicles according to current (or predicted) traffic conditions of the highway system. The link-layer control system then adjusts target speed and lane location assignment in response to real-time incidents and local traffic demand. The speed and lane-change commands from these two higher layers are then followed by the regulation-layer (AVCS) control systems as much as possible under local safety and ride quality constraints. It appears that ATMS systems are responsible for the overall traffic efficiency at the macroscopic-level, usually in an open-loop optimization manner. The link-layer control systems are responsible for coordinating the traffic flow in smaller regions using feedback control with relatively long sampling time (in the order of seconds). AVCS systems, with much higher sampling rate (milliseconds), serve as the servo mechanisms at the lowest level. We will use the acronym ATCS (advanced traffic coordination systems) to refer to the link-layer control system proposed in this paper.

The link-layer control system perceived in an earlier study by Rao and Varaiya (1994) is a traffic assignor which performs the so-called path and congestion control. The vehicle lane trajectory and target speed are assigned according to a set of heuristic rules. And the control algorithm is basically open-loop. Fenton et al. (1980) briefly described the perceived role of the regional control system in his AHS architecture, but did not present anything beyond conceptual descriptions. Ramaswamy et al. (1994) presented a lane assignment algorithm which is obtained from open-loop solution of both linear and nonlinear programming techniques. It appears fair to state that the potential of link-layer control systems on improving highway safety and efficiency has not been fully recognized and/or explored in the past. In this paper, we propose a closed-loop control algorithm which manipulates vehicle speed and lane assignment responding to real-time traffic demand/incidents.

The benefits of ATCS control schemes can be understood by examining an interesting phenomenon of human controlled traffic dynamics: when the traffic is nearly saturated, a lot of stop-and-go's may occur. These oscillatory motions propagate along the highway with small damping. This underdamped behavior arises from the neuromuscular delay and subsequent over-reaction of human drivers. Effects of exogenous disturbances (e.g., entry/exit, merge, close cut-ins) will thus stay on the highway for a long time. If all the vehicles are controlled by a central traffic control unit utilizing downstream (preview) traffic information, the vehicles should be able to move at a slow but uniform speed.

In a previous paper (Peng, 1995), the effectiveness of an ATCS algorithm has been examined against pure manual control strategies. It was found from simulation studies that the optimal ATCS algorithm uses downstream traffic status as preview information for control of upstream traffic. The simulation model is based on macroscopic traffic dynamics with number of vehicles and average speed of vehicles in cells as state variables. The phase lead inherent in the preview information improves the system damping significantly. In this paper, we have developed a computer simulation tool which keeps track of the motion of each and every vehicle on the highway. Therefore, it becomes possible to conduct more realistic simulation studies. The vehicles are assumed to be commanded by both AVCS and ATCS control strategies. The AVCS strategy calculates the control command necessary to maintain a safe spacing between vehicles locally and initiates lane changes when large density gradient is detected between adjacent lanes. The overall acceler-

Contributed by the Dynamic Systems and Control Division for publication in the JOURNAL OF DYNAMIC SYSTEMS, MEASUREMENT, AND CONTROL. Manuscript received by the DSCD August 23, 1995. Associate Technical Editor: G. Rizzoni.

ation commands to individual vehicles are obtained simply by adding the ATCS and AVCS commands.

2 Modeling

The dynamic system to be controlled consists of the vehicles on a stretch of highway. Each lane of the highway is assumed to be divided into sections (cells) of equal length. Within each section, proper sensors (e.g., video cameras) and actuation mechanisms (e.g., communication beacons on the roadside) are assumed to be available. The vehicles are assumed to be under automatic control and thus will follow the control command faithfully (under safety constraint). The traffic information collected by the sensors are assumed to be available to all the vehicles in the same link, so that the control strategy could use "global" information to calculate the control signal for each cell. Since the sensors and actuators are fixed on the highway, the control commands are assigned to the roadway sections, rather than to individual vehicles.

In this study, two traffic models are developed. A microscopic simulation model was developed to perform accurate numerical simulations. The motions of all vehicles are recorded. Each of the vehicles are assumed to be equipped with a regulation-layer vehicle controller. The main goal of the regulation-layer controller is to guarantee safe operations of individual vehicles, and follow the commands from the link-layer controller as close as possible. A macroscopic model was derived based on the well-known single-lane model (Papageorgiou, 1983) with proper modifications to include the effect of lane-changes for multiple-lane cases.

2.1 Microscopic Model. In the microscopic traffic model, the status of all the vehicles on the highway is simulated and recorded. It is assumed that the commands from the macroscopic level (ATCS) control algorithm will be followed as close as possible, subject to local safety constraints. These safety concerns are addressed by local operational rules described in the following:

(i) No vehicles are to exceed the maximum allowable speed.
(ii) It is assumed that the platooning strategy is not explicitly adopted. Rather, a constant safe "time gap" (measured in seconds) is maintained between vehicles.
(iii) The longitudinal control law at the regulation layer is assumed to be a simple P-control algorithm. The acceleration command is obtained from proportional gains multiplying range and range rate error signals. Different gains are used for accelerating and braking cases.
(iv) If no vehicle is in sight, the maximum allowable speed within that particular cell will be followed.
(v) Upon generation, each vehicle is assigned a destination exit. Lane changes will be initiated if (1) a vehicle is close to its destination point, or (2) when the traffic density of a cell is much higher than those of its neighboring cells in adjacent lanes. In the later case, the vehicles with farthest (or nearest) destination will get the highest priority for lane changes. The decision from rule 2 can be overridden by that from rule 1.
(vi) If the vehicle speed of the target lane is much higher than that of the original lane, no lane changes are allowed.
(vii) When a lane change maneuver is desired and allowed, a free spot will be generated by slowing down the vehicle in the target lane slightly. The lane change will be performed once a safe gap has been generated. During lane changes, the vehicle immediately follow the free spot cannot initiate another lane change request itself.
(viii) The vehicles will try to operate within a certain acceleration and jerk limits, except under emergency braking conditions.

These rules describe the behavior of the vehicles when the ATCS control algorithm is not in place. With ATCS, the overall acceleration of individual vehicle is equal to the summation of the acceleration command from the microscopic-level P-control plus the ATCS command. Also, lane changes can also be initiated by the ATCS controller under the same constraints as in the non-ATCS case.

2.2 Macroscopic Model. The macroscopic model is a crude but simple representation of the traffic dynamics, based on which the control algorithms can be designed. In this model, the number and the average speed of vehicles inside each cell are used as state variables, and are denoted as $n_{l,s}$ and $v_{l,s}$, respectively. The subscript l and s are the lane and section numbers of the cell, where $l = 1, \ldots NL$ ($l = 1$ for the lane on the far right) and $s = 1, \ldots NS$ ($s = 1$ for the section at the far upstream). Let $u_{l,s}n_{l,s}$ and $d_{l,s}n_{l,s}$ ($0 \le u_{l,s}, d_{l,s} \le 1$) denote the desired number of lane-changes from the (l, s) cell to the $(l + 1)$th and $(l - 1)$th lanes within one lateral control sampling time T, we have

$$\begin{aligned} n_{l,s}(k+1) = n_{l,s} &+ \frac{T}{L} v_{l,s-1} n_{l,s-1}(1 - u_{l,s-1} - d_{l,s-1}) \\ &- \frac{T}{L} v_{l,s} n_{l,s}(1 - u_{l,s} - d_{l,s}) + \frac{T}{L} v_{l+1,s-1} n_{l+1,s-1} d_{l+1,s-1} \\ &+ d_{l+1,s} n_{l+1,s}\left(1 - \frac{T}{L} v_{l+1,s}\right) - u_{l,s} n_{l,s} \\ &+ \frac{T}{L} v_{l-1,s-1} n_{l-1,s-1} u_{l-1,s-1} - d_{l,s} n_{l,s} \\ &+ u_{l-1,s} n_{l-1,s}\left(1 - \frac{T}{L} v_{l-1,s}\right) \quad (1) \end{aligned}$$

where for $l = NL$, we do not have the 3rd–6th terms, and for $l = 1$ we do not have the 7th–10th terms. It should be noted that all the state and control variables on the right hand side of Eqs. (1)–(3) are at time k, and the time index has been dropped for clarity. This is true for the following two equations as well. Equation (1) is further simplified by assuming that the following two groups of variables are small: T/L, and lane change ratios $u_{l,s}$ and $d_{l,s}$. Those terms with two or more of these variables multiplying together are neglected. Under this assumption, Eq. (1) reduces to:

$$\begin{aligned} n_{l,s}(k+1) = n_{l,s} &+ \frac{T}{L} v_{l,s-1} n_{l,s-1} - \frac{T}{L} v_{l,s} n_{l,s} \\ &+ d_{l+1,s} n_{l+1,s} - u_{l,s} n_{l,s} + u_{l-1,s} n_{l-1,s} - d_{l,s} n_{l,s} \quad (2) \end{aligned}$$

Instead of the complex equations derived in an earlier paper (Peng, 1995), the speed dynamics is assumed to be:

$$\begin{aligned} v_{l,s}(k+1) = v_{l,s} &+ a_{l,s} \cdot T + \frac{T}{\tau}[ve_{l,s} - v_{l,s}] \\ &+ \frac{T}{L} v_{l,s-1}(v_{l,s-1} - v_{l,s}) \quad (3) \end{aligned}$$

where $a_{l,s}$ denotes the acceleration command from the macroscopic-controller for the (l, s) cell. T is the sampling time, and τ is the time constant of the speed correction from the vehicle-level controller (determined by the P-gains of the microscopic-controller). $ve_{l,s}$ is the "equilibrium speed" of the cell, which

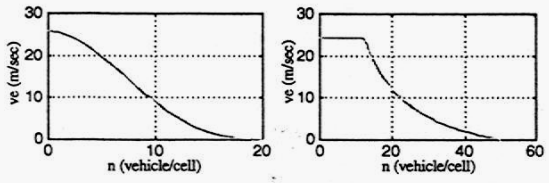

Fig. 1 Equilibrium speed under (*a*) manual and (*b*) automated control

is a function of the number of vehicles in the cell. Figure 1(*a*) shows the equilibrium speed of manual driving traffic (Cremer and May, 1985) described by the following equation

$$ve_{l,s} = V_{\max}\left[1 - \left(\frac{n_{l,s}}{n_{\max}}\right)^{m_1}\right]^{m_2}$$

where m_1 and m_2 were found to be 1.86 and 4.05, respectively, in their study. The unit of n has been normalized to become number of vehicles per 200-meter (the length of a cell used this paper). For the system we are investigating, $ve_{l,s}$ represent the equilibrium speed that will be reached by the microscopic-controller when it is working alone (without link-layer control). Under the assumption of constant time-gap of 0.5 second, maximum speed of 24.5 m/s (=55 mi/hr), and assuming that the average of the minimum spacing occupied by the vehicles (when the vehicles are stopped) is 4 m, the equilibrium speed was plotted as shown in Figure 1(*b*).

It should be noted that Eq. (3) was obtained by combining the results of Payne (1971) and Peng (1995). The "anticipatory term" in Payne is eliminated, and the anticipatory effect should come from the acceleration command $a_{l,s}(k) \cdot T$ if the macroscopic control algorithm was designed properly. The convection term (last term in Eq. (3)) was modified based on the results from a previous paper (Peng 1995).

We made another major assumption in the development of Eq. (3); i.e., lane changes do not generate large perturbations to vehicle speeds. This assumption is justified because of the local operational rules (vi) and (vii) described in Section 2.1.

3 Optimal Control Design

The nonlinear link-layer control problem was first formulated and solved using optimal control techniques. The cost functional was selected to be

$$J = \sum_{k=0}^{N-1} \tfrac{1}{2}[\underline{x}(k)^T Q \underline{x}(k) + \underline{u}(k)^T R \underline{u}(k)]$$
$$= \sum_{k=0}^{N-1} \tfrac{1}{2}[\sum_{l=1}^{NL}\sum_{s=1}^{NS}(-n_{l,s}v_{l,s}) + \sum_{l=1}^{NL}\sum_{s=1}^{NS}\rho q(u_{l,s}^2 + d_{l,s}^2) + \rho a_{l,s}^2] \quad (4)$$

where the first term represents the goal to maximize traffic flow. The other two terms represent the penalty on control signals. $\underline{x}(k)$ and $\underline{u}(k)$ represent state and control vector, respectively. They are arranged in the following order:

$$\underline{x}^T = [n_{1,1}n_{2,1}\cdots n_{NL,1}n_{1,2}\cdots n_{NL,2}\cdots n_{1,NS}\cdots n_{NL,NS}v_{1,1}v_{2,1}\cdots v_{NL,1}v_{1,2}\cdots v_{NL,2}\cdots v_{1,NS}\cdots v_{NL,NS}]$$

$$\underline{u}^T = [u_{1,1}\cdots u_{NL-1,1}u_{1,2}\cdots u_{NL-1,2}\cdots u_{NL-1,NS}d_{2,1}\cdots d_{NL,1}d_{2,2}\cdots d_{NL,2}\cdots d_{NL,NS}a_{1,1}a_{2,1}\cdots a_{NL,1}a_{1,2}\cdots a_{NL,2}\cdots a_{1,NS}\cdots a_{NL,NS}]$$

The weighting matrices Q and R are

$$Q = \begin{bmatrix} 0_{NL\cdot NS\times NL\cdot NS} & -I_{NL\cdot NS\times NL\cdot NS} \\ 0_{NL\cdot NS\times NL\cdot NS} & 0_{NL\cdot NS\times NL\cdot NS} \end{bmatrix}$$

$$R = \rho\begin{bmatrix} qI_{2(NL-1)\cdot NS\times 2(NL-1)\cdot NS} & 0_{2(NL-1)\cdot NS\times NL\cdot NS} \\ 0_{NL\cdot NS\times 2(NL-1)\cdot NS} & I_{NL\cdot NS\times NL\cdot NS} \end{bmatrix} \quad (5)$$

respectively. In the following, we will formulate the optimal control problem as one without inequality constrains. And the control algorithm is then implemented in a clipped-optimal way in the simulations with the following two inequality constraints: maximum speed, and control signal saturation. If we denote the co-state vector as

$$\lambda^T = [\lambda_{n,1,1}, \lambda_{n,2,1}, \ldots, \lambda_{n,NL,1}, \ldots, \lambda_{n,1,NS}, \ldots, \lambda_{n,NL,NS}, \lambda_{v,1,1}, \lambda_{v,2,1}, \ldots, \lambda_{v,NL,1}, \ldots, \lambda_{v,1,NS}, \ldots, \lambda_{v,NL,NS}]$$

The optimal control law can then be solved by following standard dynamic programming techniques (Bryson and Ho, 1975). Define the Hamiltonian to be $H \equiv \frac{1}{2}x^TQx + \frac{1}{2}u^TRu + \lambda^T f$, where f is the traffic dynamics ($x(k+1) = f(x(k), u(k))$) shown in Eqs. (1) and (3), the control algorithm will then become

$$u^T = -R^{-1}\lambda(k+1)^T \frac{\partial f}{\partial u}$$

where

$$\lambda(k)^T = \frac{\partial H(k)}{\partial x(k)} = x(k)^T Q + \lambda(k+1)^T \frac{\partial f}{\partial x}$$

Substitute Q and R matrices presented in Eq. (5), and system dynamics Eqs. (2) and (3), the control algorithms become:

$$u_{l,s} = \frac{-1}{\rho q}[n_{l,s}(\lambda_{n,l+1,s} - \lambda_{n,l,s})] \quad (6)$$

$$d_{l,s} = \frac{-1}{\rho q}[n_{l,s}(\lambda_{n,l-1,s} - \lambda_{n,l,s})] \quad (7)$$

$$a_{l,s} = \frac{-T\cdot\lambda_{v,1,s}}{\rho} \quad (8)$$

where the co-state equations are

$$\lambda_{n,l,s}(k) = \left[1 - \frac{T}{L}v_{l,s} - u_{l,s} - d_{l,s}\right]\lambda_{n,l,s} + \frac{T}{L}v_{l,s}\lambda_{n,l,s+1} + d_{l,s}\lambda_{n,l-1,s} + u_{l,s}\lambda_{n,l+1,s} - v_{l,s} \quad (9)$$

$$\lambda_{v,l,s}(k) = \frac{T}{L}n_{l,s}(\lambda_{n,l,s+1} - \lambda_{n,l,s}) + \left(1 - \frac{T}{\tau} - \frac{T}{L}v_{l,s-1}\right)\lambda_{v,l,s} + \frac{T}{L}(2v_{l,s} - v_{l,s+1})\lambda_{v,l,s+1} \quad (10)$$

where all the co-state variables on the right hand side of Eqs. (9) and (10) are at time $(k+1)$, and the time indices have been dropped to make the equations easier to follow. The true optimal solution involves simultaneously solving the state equations (Eq. (2) and (3)) and co-state equations (Eqs. (9) and (10)) and are usually done in an iterative fashion.

4 Distributed Control Algorithm

In a previous publication (Peng, 1995), we have studied the possibility of implementing a true nonlinear optimal control algorithm similar to the one presented in Section 3. Macroscopic simulation results for several non-ideal traffic conditions for both single-lane and two-lane cases were presented. It was

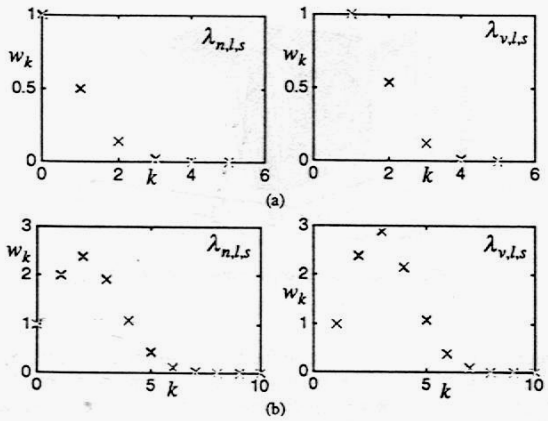

Fig. 2 Normalized weighting factors of the downstream traffic information for (*a*) V = 20 m/s and (*b*) V = 40 m/s

found that the recursive solution of the two point boundary value problems (TPBVP) is sensitive to numerical settings. Furthermore, the final control algorithm is in a rigorous but complicated form. When a control designer adjusts the weighting matrices, the results may be subject to numerical difficulty arises mainly from the iterative two-point-boundary-value solution process. Another drawback of the true optimal control algorithm (i.e., solution of the TPBVP) is that the controller requires global information feedback. We believe that looking forward for more than a certain distance will bring no extra benefits. In other words, a distributed control algorithm which looks forward for a finite distance should work. Because of the two reasons mentioned above, we propose a decentralized control algorithm, which is based on a simplified version of the optimal control method presented in the previous section. The new control law is in a distributed form and thus can be implemented more easily.

We noticed that the co-state $\lambda_{n,l,s}$ in Eq. (9) can be viewed as a dynamic equation with vehicle speed as the excitation input. It also allows the dynamics of downstream and sideways cells to propagate toward upstream cells. The weighting given to the downstream cell state (more precisely, co-state) is proportional to $(T/L)v_{l,s}$. In other words, when the control sampling time becomes larger, or when the vehicle speed increases, the coupling from downstream cells to upstream cells will increase. In essence, we could interpret the costate $\lambda_{n,l,s}$ as filtered vehicle speed at that particular cell over time. The extra terms then represent the consideration of "flow rate difference" from neighboring cells due to traffic flow and lane changes.

To develop a distributed control law, we have to separate the forward (x) and backward (λ) dynamics. To carry out this engineering approximation, we choose to fix the state variables at their current values when we calculate the backward dynamics. This assumption was referred to as "pseudo-steady-state"

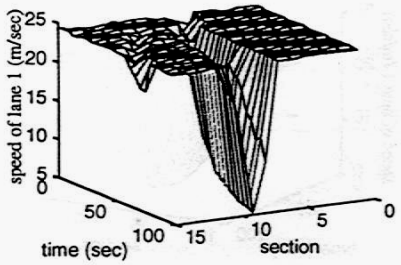

Fig. 3 Uneven traffic smooth-out (w/o ATCS)

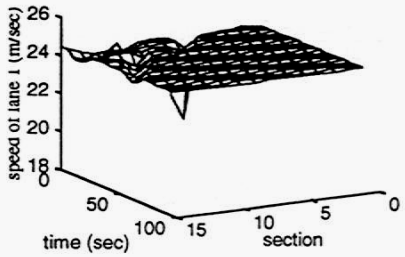

Fig. 4 Uneven traffic smooth-out (with ATCS)

in the following derivation. It should be noted that under this assumption, we are solving an approximated (near-optimal?) problem. Integrate Eq. (9) k steps assuming pseudo-steady-state condition and neglect the lane-changing terms, we have

$$\lambda_{n,l,s} = -kv_{l,s} + \frac{k(k-1)}{2!}\frac{T}{L}v_{l,s}(-v_{l,s+1} + v_{l,s}) + \frac{k(k-1)(k-2)}{3!}\left(\frac{T}{L}\right)^2 v_{l,s}v_{l,s+1}(-v_{l,s+2} + v_{l,s+1}) + \frac{k(k-1)(k-2)(k-3)}{4!}\left(\frac{T}{L}\right)^3 \times v_{l,s}v_{l,s+1}v_{l,s+2}(-v_{l,s+3} + v_{l,s+2}) + \cdots + k\left(\frac{T}{L}\right)^{k-2} v_{l,s}v_{l,s+1}v_{l,s+2}\cdots v_{l,s+k-3}(-v_{l,s+k-2} + v_{l,s+k-3}) + \left(\frac{T}{L}\right)^{k-1} v_{l,s}v_{l,s+1}v_{l,s+2}\cdots v_{l,s+k-2}(-v_{l,s+k-1} + v_{l,s+k-2}) \quad (11)$$

In other words, the lane change control schemes (Eqs. (6) and (7)) can be interpreted to have the following physical meaning: a weighted speed and speed difference between local cell and downstream cells are first calculated based on Eq. (11). This weighted speed term is then multiplied by the number of vehicles to generate an "expected flow rate difference" between cells. If a cell has a lower expected flow over the foreseeable horizon than its neighboring cells, a portion of the vehicles will be directed to the faster neighboring lane(s). Furthermore, the lane change ratio will be proportional to the expected flow rate difference between the two lanes (see Eqs. (6) and (7)). Similarly, we integrate Eq. (10) for k steps under the pseudo-steady-state condition, and we have

$$\lambda_{v,l,s} = \frac{T}{L}\left[\frac{k(k-1)}{2!}n_{l,s}(-v_{l,s+1} + v_{l,s}) + \frac{k(k-1)(k-2)}{3!}\frac{T}{L}v_{l,s+1}n_{l,s}(-v_{l,s+2} + v_{l,s+1}) + \frac{k(k-1)(k-2)}{3!}\frac{T}{L}(2v_{l,s} - v_{l,s+1})n_{l,s+1}(-v_{l,s+2} + v_{l,s+1})\right.$$

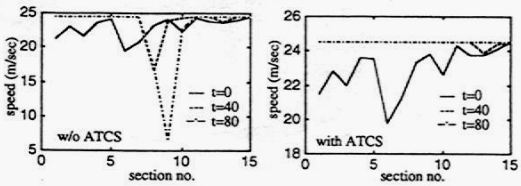

Fig. 5 Selected speed history for uneven traffic case

$$+\frac{k(k-1)(k-2)(k-3)}{4!}\left(\frac{T}{L}\right)^2 \times v_{l,s+1}v_{l,s+2}n_{l,s}(-v_{l,s+3}+v_{l,s+2})$$

$$+\frac{k(k-1)(k-2)(k-3)}{4!}\left(\frac{T}{L}\right)^2$$

$$\times (2v_{l,s}-v_{l,s+1})v_{l,s+2}n_{l,s+1}(-v_{l,s+3}+v_{l,s+2})$$

$$+\frac{k(k-1)(k-2)(k-3)}{4!}\left(\frac{T}{L}\right)^2$$

$$\times (2v_{l,s}-v_{l,s+1})(2v_{l,s+1}-v_{l,s+2})n_{l,s+2}(-v_{l,s+3}+v_{l,s+2})+\cdots$$

$$+\left(\frac{T}{L}\right)^{k-2} v_{l,s+1}\cdots v_{l,s+k-2}n_{l,s}(-v_{l,s+k-1}+v_{l,s+k-2})$$

$$+\left(\frac{T}{L}\right)^{k-2}(2v_{l,s}-v_{l,s+1})v_{l,s+2}\cdots \times v_{l,s+k-2}n_{l,s+1}(-v_{l,s+k-1}+v_{l,s+k-2})$$

$$+\left(\frac{T}{L}\right)^{k-2}(2v_{l,s}-v_{l,s+1})(2v_{l,s+1}-v_{l,s+2})v_{l,s+3}\cdots$$

$$\times v_{l,s+k-2}n_{l,s+2}(-v_{l,s+k-1}+v_{l,s+k-2})+\left(\frac{T}{L}\right)^{k-2}(2v_{l,s}-v_{l,s+1})\cdots$$

$$\times (2v_{l,s+k-3}-v_{l,s+k-2})n_{l,s+k-2}(-v_{l,s+k-1}+v_{l,s+k-2})\Bigg] \quad (12)$$

The interpretation of the acceleration control algorithm shown in Eq. (8) is as following: A weighted expected flow rate difference will be calculated for each cell by following Eq. (12). The expected flow rate is obtained by multiplying traffic density (e.g., $n_{l,s+1}$) in the downstream cells with speed gradient terms (e.g. $(-v_{l,s+k-1}+v_{l,s+k-2})$. Furthermore, the weighting coefficients (e.g. $k!/k!(T/L)^{k-2}(2v_{l,s}-v_{l,s+1})v_{l,s+2}\cdots v_{l,s+k-2}$) are speed and sampling-time dependent. This weighted flow rate difference determines whether the expected flow rate in the local cell should be lowered or increased. Again, the acceleration will be proportional to this weighted expected flow rate difference.

It can be seen that both Eqs. (11) and (12) describe distributed control algorithms. By using state variables of local cell and a finite number of downstream cells, the control commands can be computed. Furthermore, downstream traffic flow status has been used as preview information for the control of upstream cells. The weighting factors of the preview terms in Eqs. (11) and (12) can be interpreted as the relative importance of the future information of the downstream cells in computing the distributed control signals. Let w_k denotes the sum of the weighting coefficients of the terms containing at the maximum the information of the kth downstream cell. It can be seen from Figure 2(*a*) that when the vehicle speed is low, w_k decays exponentially for both Eqs. (11) and (12). When the vehicle speed is high, traffic information in some of the future downstream cells may be given a larger weighting than the immediate downstream cell. Figure 2 was obtained by assuming the following values: $T = 2$ s, $L = 200$ m, and a preview time of 50 seconds, which is used to determine the maximum k. Figure 2 suggests that a preview time of 30–40 seconds seems to be enough. However, this analysis is obtained purely based on the macroscopic model. When ride quality and effect of lane changes to traffic speed perturbation are included, it was judged from the simulation results that preview of 50–60 seconds seems more appropriate for operations under normal highway speeds.

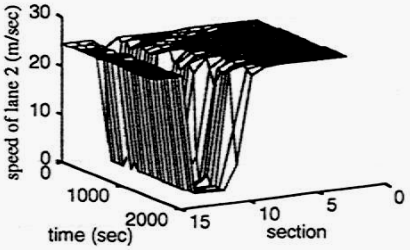

Fig. 7 One car broken-down (with ATCS)

5 Simulation Results

In the simulations, the traffic is assumed to be created at the upstream (section 0) by a random binomial generator. A "congestion ratio" is used to determine the number of vehicles in section zero. A congestion ratio of 1.0 denotes that the number of vehicles is equal to the corner point shown in Fig. 1(*b*). When congestion ratio is larger than 1.0, the vehicles will have to operate at a lower speed, also determined by the n-v relationship shown in Fig. 1(*b*). A 3 km-long stretch of 3-lane highway is simulated. Each lane is assumed to be divided into 15 cells of 200 m each. The maximum vehicle speed is assumed to be 24.5 m/s (55 mi/hr). Control sampling time $T = 2$ s, and it was assumed that the control algorithm look ahead for 5 cells. Transient response under three kinds of perturbed conditions were examined: (1) nonuniform traffic density and speed under near-saturated condition; (2) one broken-down vehicle in the middle lane; and (3) continuous traffic merging from the right-hand side lane.

Figures 3 and 4 show the results simulating the transient response under uneven traffic distribution. The highway is assumed to be nearly saturated (congestion ratio = 0.75). The unevenness may arise from entry/exit or other perturbations. In the beginning of the simulations, the vehicle speed and number of vehicles in the cells are generated randomly with a standard deviation of 2.3 m/sec. While the microscopic P-control algorithm has some inherent damping (Kp for range error = 0.1, *Kd* for range rate error = 0.2), in this particular case it is not enough to smooth out the traffic. Figure 5 shows that when the initial nonuniformity of the traffic is large enough (around section 6), a worse gridlock may occur in the non-ATCS case. In

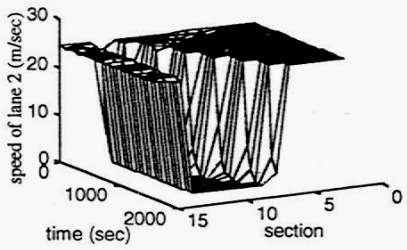

Fig. 6 One car broken-down (w/o ATCS)

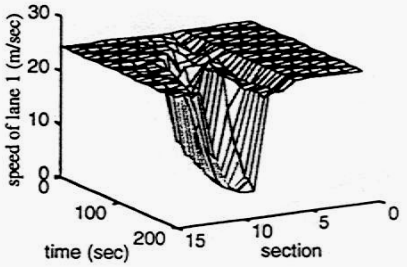

Fig. 8 Merging traffic (w/o ATCS)